NON-LINEAR PERISTALTIC FLOW OF WALTER'S B FLUID IN AN ASYMMETRIC CHANNEL WITH HEAT TRANSFER AND CHEMICAL REACTIONS

by

Obaid Ullah MEHMOOD [a,b], Norzieha MUSTAPHA [a,*], and Sharidan SHAFIE [a]

[a] Department of Mathematics, Faculty of Science, University of Technology Malaysia, Johor Bahru, Malaysia
[b] COMSATS Institute of Information Technology, Wah Cantt, Pakistan

Original scientific paper
DOI: 10.2298/TSCI110921096M

In this paper, effects of heat and mass transfer on peristaltic transport of Walter's B fluid in an asymmetric channel are investigated. The governing equations are solved using regular perturbation method by taking wave number as a small parameter. Expressions for the stream function, temperature distribution, heat transfer coefficient, and mass concentration are presented in explicit form. Solutions are analyzed graphically for different values of arising parameters such as viscoelastic parameter, Prandtl, Eckert, Soret, Schmidt, and Reynolds number. It has been found that these parameters considerably affect the considered flow characteristics. Results show that with an increase in Eckert and Prandtl number temperature and heat transfer coefficient increase while mass concentration decreases. Further, Mass concentration also decreases with increasing Soret and Schmidt number.

Key words: *peristaltic flow, Walter's B fluid, heat and mass transfer, Soret effects, viscous dissipation*

Introduction

Peristalsis is a natural mechanism of fluid motion inside the living tracts induced by the wavy motion of the tract boundaries. This wavy motion is sinusoidal in nature [1] and responsible for mixing and transportation of contents with in the tubes. The examples found in the living body include motion of food in the gastrointestinal tract, motion of secretions in glandular ducts, transport of urine in the cervical canal and others. In industrial applications, it is involved in artificial heart and ortho-pumps, heart lung machines, transport of toxic material, waste inside the sanitary ducts and others. The mentioned situations usually involve the fluid having non-Newtonian behaviour with some elastic characteristics because most of them are the suspension of particles in Newtonian fluid with fading memory. Walter's B fluid model with limiting viscosity at low shear rates and short memory coefficient [2] is the best model for mentioned situations as discussed in literature [3-9].

It is evident from the work of Vries *et al*. [10] that the intrauterine fluid flow with myometrial contractions is asymmetric in nature. Also, nonpregnant uterus exhibits contractions with variable amplitudes, frequencies and wavelengths [11]. These facts prompt to con-

* Corresponding author; e-mail: norzieha@utm.my

sider the asymmetric configuration in the present problem. Because of the intricate nature of the biofluid dynamics, both heat and mass transfer occur simultaneously giving complex relations between fluxes and driving potentials examples oxygenation of blood, hemodialysis, heat conduction in tissues, heat transfer due to perfusion of arterial-venous blood, metabolic processes involved in digestion of food and others. Mostly, the fluid flow is governed by the temperature gradient or composition gradient. When the mass flux is caused by the temperature gradient, it is called Soret effects (thermal-diffusion). Soret effects are used for the separation of isotopes. These effects are often negligible in heat and mass transfer analysis, but for the fluids with light (helium) or medium (air) molecular weights, it is not appropriate to neglect these effects [12, 13].

Much attention has been paid on heat and mass transfer analysis of Newtonian fluid [14-19]. Muthuraj and Srinivas [20] studied mixed convective heat and mass transfer in a vertical porous channel. They considered the MHD viscous fluid flow induced by thermal waves. They obtained solutions comprising of two parts namely: mean solution and perturbed solution, using regular perturbation method. Srinivas *et al.* [21] considered the mixed convective heat and mass transfer on peristaltic flow of viscous fluid in a vertical asymmetric channel. They linearized the governing equations in wave frame assuming long wavelength. Then, they obtained analytical solutions about small wave number using perturbation method. They considered Soret and Dufour effects in their investigation. Srinivas *et al.* [22] extended the work of Srinivas *et al*. [21] by investigating the effects of space porosity and chemical reactions on mixed convective heat and mass transfer of MHD peristaltic transport. They considered the flow of viscous fluid through a vertical porous asymmetric channel. They followed the similar approach for solutions but neglected the Soret and Dufour effects in this problem. A detailed study on thermal-diffusion and diffusion-thermo effects on the flow of viscous fluid is conducted by Srinivas *et al*. [23]. They considered the flow between two slowly contracting and expanding weakly permeable, porous walls. They linearized the governing equations by assuming symmetric injection or suction and similarity transformations. Following Berman's classic approach, they obtained solutions using perturbation method twice, first for small permeation Reynolds number and second for small wall dilation parameter.

Because of the different rheological properties of non-Newtonian fluids, there is no single constitutive relationship between stress and rate of strain by which all the non-Newtonian fluids can be examined. Therefore, several models of non-Newtonian fluids have been suggested and considered. Heat and mass transfer on peristaltic flow of different non-Newtonian fluid models have been studied by [24-26]. Recently, peristaltic flow of hyperbolic tangent fluid in an annulus with heat and mass transfer is studied by Akbar *et al.* [27]. They obtained both analytical and numerical solutions under long wavelength approximation. Nadeem and Akbar [28] studied the effects of induced MHD and heat and mass transfer on peristaltic transport of Segalman fluid in an asymmetric vertical channel. They obtained the solutions by three different methods: perturbation method, homotopy analysis method, and shooting method. Hayat and Hina [29] investigated the effects of slip and compliant walls on heat and mass transfer of peristaltic flow of Williamson fluid in a non-uniform channel. Their solutions are valid for small Wissenberg number. However, to the best of our knowledge, no one investigated the effects of heat and mass transfer on peristaltic flow of Walter's B fluid in an asymmetric channel which is of considerable interest in physiological and industrial research. Motivated by the facts discussed above, in the present problem, peristaltic flow of Walter's B fluid in an asymmetric channel with heat and mass transfer is addressed. In addition, viscous dissipation and Soret effects are given due attention. The governing equations are solved adopting long wavelength and small Reynolds number approximations. Finally, the results are graphically presented and discussed for several pertinent parameters.

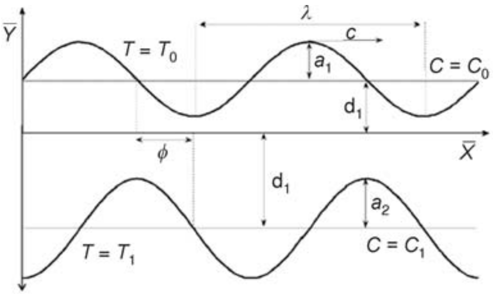

Figure 1. Sketch of the physical model

Formulation of the problem

2-D flow of an incompressible Walter's B fluid in an asymmetric channel is considered. The fluid is caused to flow due to the sinusoidal waves of different amplitudes and phases moving along the channel walls with constant speed c. The upper and lower walls are at distance d_1 and d_2 from the centerline ($\bar{Y} = 0$) of the channel. The upper wall is maintained at temperature T_0 and lower wall is maintained at temperature T_1, respectively. The sketch of the physical model is given in fig. 1.

Under these assumptions the continuity, momentum, energy, and concentration equations are:

$$\frac{\partial \bar{U}}{\partial \bar{X}} + \frac{\partial \bar{V}}{\partial \bar{Y}} = 0 \tag{1}$$

$$\rho\left(\frac{\partial}{\partial t} + \bar{U}\frac{\partial}{\partial \bar{X}} + \bar{V}\frac{\partial}{\partial \bar{Y}}\right)\bar{U} = -\frac{\partial \bar{P}}{\partial \bar{X}} + \frac{\partial \bar{S}_{\bar{X}\bar{X}}}{\partial \bar{X}} + \frac{\partial \bar{S}_{\bar{X}\bar{Y}}}{\partial \bar{Y}} \tag{2}$$

$$\rho\left(\frac{\partial}{\partial t} + \bar{U}\frac{\partial}{\partial \bar{X}} + \bar{V}\frac{\partial}{\partial \bar{Y}}\right)\bar{V} = -\frac{\partial \bar{P}}{\partial \bar{Y}} + \frac{\partial \bar{S}_{\bar{X}\bar{Y}}}{\partial \bar{X}} + \frac{\partial \bar{S}_{\bar{Y}\bar{Y}}}{\partial \bar{Y}} \tag{3}$$

$$\rho\xi\left(\frac{\partial}{\partial t} + \bar{U}\frac{\partial}{\partial \bar{X}} + \bar{V}\frac{\partial}{\partial \bar{Y}}\right)\bar{T} = k\left(\frac{\partial^2 T}{\partial \bar{X}^2} + \frac{\partial^2 T}{\partial \bar{Y}^2}\right) + \bar{\Phi} \tag{4}$$

$$\left(\frac{\partial}{\partial \bar{t}} + \bar{U}\frac{\partial}{\partial \bar{X}} + \bar{V}\frac{\partial}{\partial \bar{Y}}\right)C = D\left(\frac{\partial^2 C}{\partial \bar{X}^2} + \frac{\partial^2 C}{\partial \bar{Y}^2}\right) + \frac{DK_T}{T_m}\left(\frac{\partial^2 T}{\partial \bar{X}^2} + \frac{\partial^2 T}{\partial \bar{Y}^2}\right) \tag{5}$$

where

$$\bar{S}_{\bar{X}\bar{X}} = \eta_0(4\bar{U}_{\bar{X}}) - k_0(4\bar{U}_{\bar{X}t} + 4\bar{U}\bar{U}_{\bar{X}\bar{X}} + 4\bar{V}\bar{U}_{\bar{X}\bar{Y}} - 8\bar{U}_{\bar{X}}^2 - 4\bar{V}_{\bar{X}}\bar{U}_{\bar{Y}} - 4\bar{V}_{\bar{X}}^2) \tag{6}$$

$$\begin{aligned}\bar{S}_{\bar{X}\bar{Y}} = \eta_0(2\bar{U}_{\bar{Y}} + 2\bar{V}_{\bar{X}}) - k_0(2\bar{U}_{\bar{Y}t} + 2\bar{V}_{\bar{X}t} + 2\bar{U}\bar{U}_{\bar{X}\bar{Y}} + 2\bar{U}\bar{V}_{\bar{X}\bar{X}} + 2\bar{V}\bar{U}_{\bar{Y}\bar{Y}} + 2\bar{V}\bar{V}_{\bar{X}\bar{Y}} - 6\bar{U}_{\bar{X}}\bar{U}_{\bar{Y}} - \\ -2\bar{U}_{\bar{Y}}\bar{V}_{\bar{Y}} - 2\bar{U}_{\bar{X}}\bar{V}_{\bar{X}} - 6\bar{V}_{\bar{X}}\bar{V}_{\bar{Y}}\end{aligned} \tag{7}$$

$$\bar{S}_{\bar{Y}\bar{Y}} = \eta_0(4\bar{V}_{\bar{Y}}) - k_0(4\bar{V}_{\bar{Y}t} + 4\bar{U}\bar{V}_{\bar{X}\bar{Y}} + 4\bar{V}\bar{V}_{\bar{Y}\bar{Y}} - 4\bar{U}_{\bar{Y}}^2 - 4\bar{V}_{\bar{X}}\bar{U}_{\bar{Y}} - 8\bar{V}_{\bar{Y}}^2 \tag{8}$$

$$\begin{aligned}\bar{\Phi} = 4\eta_0\bar{U}_{\bar{X}}^2 - 4k_0\bar{U}_{\bar{X}}\bar{U}_{t\bar{X}} - 4k_0\bar{U}\bar{U}_{\bar{X}}\bar{U}_{\bar{X}\bar{X}} - 4k_0\bar{V}\bar{U}_{\bar{X}}\bar{U}_{\bar{X}\bar{Y}} + 8k_0\bar{U}_{\bar{X}}^3 + 12k_0\bar{U}_{\bar{X}}\bar{U}_{\bar{Y}}\bar{V}_{\bar{X}} + \\ +6k_0\bar{U}_{\bar{X}}\bar{V}_{\bar{X}}^2 + 2\eta_0\bar{U}_{\bar{Y}}^2 + 4\eta_0\bar{U}_{\bar{Y}}\bar{V}_{\bar{X}} - 2k_0\bar{U}_{\bar{Y}}\bar{U}_{t\bar{Y}} - 2k_0\bar{U}_{\bar{Y}}\bar{V}_{t\bar{X}} - 2k_0\bar{U}\bar{U}_{\bar{Y}}\bar{U}_{\bar{X}\bar{Y}} - 2k_0\bar{U}\bar{U}_{\bar{Y}}\bar{V}_{\bar{X}\bar{X}} - \\ -2k_0\bar{V}\bar{U}_{\bar{Y}}\bar{U}_{\bar{Y}\bar{Y}} - 2k_0\bar{V}\bar{U}_{\bar{Y}}\bar{V}_{\bar{X}\bar{Y}} + 6k_0\bar{U}_{\bar{X}}\bar{U}_{\bar{Y}}^2 + 6k_0\bar{U}_{\bar{Y}}^2\bar{V}_{\bar{Y}} + 12k_0\bar{U}_{\bar{Y}}\bar{V}_{\bar{Y}}\bar{V}_{\bar{X}} + 2\eta_0\bar{V}_{\bar{X}}^2 - 2k_0\bar{V}_{\bar{X}}\bar{U}_{t\bar{Y}} - \\ -2k_0\bar{V}_{\bar{X}}\bar{V}_{t\bar{X}} - 2k_0\bar{U}\bar{V}_{\bar{X}}\bar{U}_{\bar{X}\bar{Y}} - 2k_0\bar{U}\bar{V}_{\bar{X}}\bar{U}_{\bar{X}\bar{X}} - 2k_0\bar{V}\bar{V}_{\bar{X}}\bar{U}_{\bar{Y}\bar{Y}} - 2k_0\bar{V}\bar{V}_{\bar{X}}\bar{V}_{\bar{X}\bar{Y}} + 6k_0\bar{V}_{\bar{X}}^2\bar{V}_{\bar{Y}} + 4\eta_0\bar{V}_{\bar{Y}}^2 - \\ -4k_0\bar{V}_{\bar{Y}}\bar{V}_{t\bar{Y}} - 4k_0\bar{U}\bar{V}_{\bar{Y}}\bar{V}_{\bar{X}\bar{Y}} - 4k_0\bar{V}\bar{V}_{\bar{Y}}\bar{V}_{\bar{Y}\bar{Y}} + 8k_0\bar{V}_{\bar{Y}}^3\end{aligned} \tag{9}$$

with boundary conditions and geometries of the channel walls $\overline{H}_1$ and $\overline{H}_2$:

$$\overline{U}=0,\quad T=T_0,\quad C=C_0,\quad \text{at}\quad \overline{Y}=\overline{H}_1 \tag{10}$$

$$\overline{U}=0,\quad T=T_1,\quad C=C_1,\quad \text{at}\quad \overline{Y}=\overline{H}_2 \tag{11}$$

$$\overline{H}_1(\overline{X},\bar{t})=d_1+a_1\sin\left[\frac{2\pi}{\lambda}(\overline{X}-c\bar{t})\right] \tag{12}$$

$$\overline{H}_2(\overline{X},\bar{t})=-d_2-a_2\sin\left[\frac{2\pi}{\lambda}(\overline{X}-c\bar{t})+\phi\right] \tag{13}$$

In the above expressions, eqs. (1)-(13), ρ is the fluid density, $\overline{P}$ – the pressure, T – the fluid temperature, C – the fluid concentration, k – the thermal conductivity, ξ – the specific heat at constant volume, T_m – the temperature of the medium, D – the coefficient of mass diffusivity, K_T – the thermal-diffusion ratio, $\overline{U}$ – the longitudinal velocity component, $\overline{V}$ – the transverse velocity component, $a_\mathrm{i}(i=1,2)$ – the wave amplitudes at upper and lower walls, λ – the wave length, $\bar{t}$ – the time and ϕ are the phase difference varying in the range $0\le\phi\le\pi$, ($\phi=0$ leads us to the symmetric channel with waves out of phase and $\phi=\pi$, the waves are in phase). Moreover, a_i, d_i, and ϕ satisfy the condition:

$$a_1^2+a_2^2+2a_1a_2\cos\phi\le(d_1+d_2)^2 \tag{14}$$

The extra stress tensor $\overline{\mathbf{S}}$ for Walter's B fluid satisfies the constitutive relationship [3], is given as:

$$\overline{\mathbf{S}}=2\eta_0\mathbf{e}-2k_0\frac{\delta\mathbf{e}}{\delta\bar{t}} \tag{15}$$

$$\frac{\delta\mathbf{e}}{\delta\bar{t}}=\frac{\partial\mathbf{e}}{\partial\bar{t}}+\mathbf{V}\nabla\mathbf{e}-\mathbf{e}\nabla\mathbf{V}-\nabla\mathbf{V}^T\mathbf{e} \tag{16}$$

where $\mathbf{e}$ is the rate of strain tensor, $\delta\mathbf{e}/\delta\bar{t}$ – the convected differentiation of rate of strain tensor in relation to the material in motion, η_0 – the limiting viscosity at small shear rates, and k_0 – the short memory coefficient.

Defining the following transformations:

$$\bar{x}=\overline{X}-\overline{ct},\quad \bar{y}=\overline{Y},\quad \bar{u}=\overline{U}-c,\quad \bar{v}=\overline{V},\quad \bar{p}=\overline{P} \tag{17}$$

and considering non-dimensional quantities:

$$x=\frac{\bar{x}}{\lambda},\ y=\frac{\bar{y}}{d_1},\ u=\frac{\bar{u}}{c},\ v=\frac{\bar{v}}{c},\ p=\frac{d_1^2}{\eta_0\lambda c}p,\ h_1=\frac{\overline{h_1}}{d_1},\ h_2=\frac{\overline{h_2}}{d_2},\ \mathbf{S}=\frac{d_1}{\eta_0 c}\overline{\mathbf{S}},\ \delta=\frac{d_1}{\lambda}$$
$$\mathrm{Re}=\frac{\rho cd_1}{\eta_0},\ \kappa=\frac{k_0c}{\eta_0d_1},\ \Phi=\frac{d_1^2}{\eta_0c^2}\overline{\Phi},\ \eta=\frac{T-T_0}{T_1-T_0},\ \mathrm{Ec}=\frac{c^2}{\xi(T_1-T_0)},\ \mathrm{Pr}=\frac{\xi\eta_0}{k}$$
$$\varphi=\frac{C-C_0}{C_1-C_0},\ \mathrm{Sc}=\frac{\eta_0}{\rho D},\ \mathrm{Sr}=\frac{\rho DK_T(T_1-T_0)}{\eta_0T_m(C_1-C_0)} \tag{18}$$

and letting the stream function Ψ related to the velocity components u and v by the relations:

$$u=\frac{\partial\Psi}{\partial y},\quad v=-\delta\frac{\partial\Psi}{\partial x} \tag{19}$$

the continuity equation is satisfied and eqs. (2)-(14) reduce to forms:

$$\delta=\mathrm{Re}\left[\left(\frac{\partial\Psi}{\partial y}\frac{\partial}{\partial x}-\frac{\partial\Psi}{\partial x}\frac{\partial}{\partial y}\right)\frac{\partial\Psi}{\partial y}\right]=\frac{\partial p}{\partial x}+\delta\frac{\partial S_{xx}}{\partial x}+\frac{\partial S_{xy}}{\partial y} \tag{20}$$

$$-\delta^3\mathrm{Re}\left[\left(\frac{\partial\Psi}{\partial y}\frac{\partial}{\partial x}-\frac{\partial\Psi}{\partial x}\frac{\partial}{\partial y}\right)\frac{\partial\Psi}{\partial x}\right]=-\frac{\partial p}{\partial y}+\delta^2\frac{\partial S_{xy}}{\partial x}+\delta\frac{\partial S_{yy}}{\partial y} \tag{21}$$

$$\delta\,\mathrm{Re}\left[\left(\frac{\partial\Psi}{\partial y}\frac{\partial}{\partial x}-\frac{\partial\Psi}{\partial x}\frac{\partial}{\partial y}\right)\nabla^2\Psi\right]=\left(\frac{\partial^2}{\partial y^2}-\delta^2\frac{\partial^2}{\partial x^2}\right)S_{xy}+\delta\frac{\partial^2}{\partial x\partial y}(S_{xx}-S_{yy}) \tag{22}$$

$$\delta\,\mathrm{Re}\left(\frac{\partial\Psi}{\partial y}\frac{\partial\eta}{\partial x}-\frac{\partial\Psi}{\partial x}\frac{\partial\eta}{\partial y}\right)=\frac{1}{\mathrm{Pr}}\left(\delta^2\frac{\partial^2\eta}{\partial x^2}+\frac{\partial^2\eta}{\partial y^2}\right)+\mathrm{Ec}\Phi \tag{23}$$

$$\delta\,\mathrm{Re}\left(\frac{\partial\Psi}{\partial y}\frac{\partial\varphi}{\partial x}-\frac{\partial\Psi}{\partial x}\frac{\partial\varphi}{\partial y}\right)=\frac{1}{\mathrm{Sc}}\left(\delta^2\frac{\partial^2\varphi}{\partial x^2}+\frac{\partial^2\varphi}{\partial y^2}\right)+\mathrm{Sr}\left(\delta^2\frac{\partial^2\eta}{\partial x^2}+\frac{\partial^2\eta}{\partial y^2}\right) \tag{24}$$

where $\nabla^2=\delta^2(\partial^2/\partial x^2)+\partial^2/\partial y^2$

$$S_{xx}=4\delta\Psi_{xy}-\kappa(4\delta^2\Psi_y\Psi_{xxy}-4\delta^2\Psi_x\Psi_{xyy}-8\delta\Psi_{xy}^2+4\delta^2\Psi_{xx}\Psi_{yy}-4\delta^4\Psi_{xx}^2) \tag{25}$$

$$\begin{aligned}S_{xy}=2(\Psi_{yy}-\delta^2\Psi_{xx})-\kappa(2\delta\Psi_y\Psi_{xyy}-2\delta^3\Psi_y\Psi_{xxx}-2\delta\Psi_x\Psi_{yyy}+2\delta^3\Psi_x\Psi_{xxy}-6\delta\Psi_{xy}\Psi_{yy}+\\+2\delta\Psi_{yy}\Psi_{xy}+2\delta^3\Psi_{xy}\Psi_{xx}-6\delta^3\Psi_{xx}\Psi_{xy})\end{aligned} \tag{26}$$

$$S_{yy}=-4\delta\Psi_{xy}-\kappa(-4\delta^2\Psi_y\Psi_{xxy}+4\delta^2\Psi_x\Psi_{xxy}-4\Psi_{yy}^2+4\delta^2\Psi_{xx}\Psi_{yy}-8\delta^2\Psi_{xy}^2) \tag{27}$$

$$\begin{aligned}\Phi=4\delta^2\Psi_{xy}^2-4\kappa\delta^2\Psi_{xy}\Psi_{xxy}+4\kappa\delta^3\Psi_x\Psi_{xy}\Psi_{xyy}+8\kappa\delta^3\Psi_{xy}^3-12\kappa\delta^3\Psi_{xy}\Psi_{yy}\Psi_{xx}+6\kappa\delta^5\Psi_{xy}\Psi_{xx}^2+\\+2\Psi_{yy}^2-4\delta^2\Psi_{yy}\Psi_{xx}-2\kappa\delta\Psi_y\Psi_{yy}\Psi_{xyy}+2\kappa\delta^3\Psi_y\Psi_{yy}\Psi_{xxx}+2\kappa\delta\Psi_x\Psi_{xx}\Psi_{yyy}+2\kappa\delta^3\Psi_x\Psi_{yy}\Psi_{xxy}+\\+6\kappa\delta\Psi_{xy}\Psi_{yy}^2-6\kappa\delta\Psi_{yy}\Psi_{xy}+2\kappa\delta^3\Psi_{yy}\Psi_{xy}\Psi_{xx}+2\delta^4\Psi_{xx}^2+2\kappa\delta^5\Psi_y\Psi_{xx}\Psi_{xyy}-2\kappa\delta^5\Psi_y\Psi_{xx}\Psi_{xxx}-\\-2\kappa\delta^3\Psi_x\Psi_{xx}\Psi_{yyy}+2\kappa\delta^5\Psi_\xi\Psi_{xx}\Psi_{xxy}+6\kappa\delta^4\Psi_{xx}\Psi_{xy}+4\delta^2\Psi_{xy}^2-4\kappa\delta^3\Psi_y\Psi_{xy}\Psi_{xxy}+\\+4\kappa\delta^3\Psi_x\Psi_{xy}\Psi_{xyy}-8\kappa\delta^3\Psi_{xy}^3\end{aligned} \tag{28}$$

with boundary conditions and wall geometries $h_1(x)$ and $\mathrm{h}_2(x)$:

$$\Psi=\frac{F}{2},\quad \frac{\partial\Psi}{\partial y}=-1,\quad \eta=0,\quad \varphi=0\quad \text{at}\quad y=h_1(x) \tag{29}$$

$$\Psi=-\frac{F}{2},\quad \frac{\partial\Psi}{\partial y}=-1,\quad \eta=1,\quad \varphi=1\quad \text{at}\quad y=h_2(x) \tag{30}$$

$$h_1(x)=1+a\sin(2\pi x)\quad \text{and}\quad h_2(x)=-d-b\sin(2\pi x+\phi) \tag{31}$$

Here, δ is the wave number, Re – the Reynolds number, κ – the viscoelastic parameter, Ec – the Eckert number, Pr – the Prandtl number, Sc – the Schmidt number, Sr – the Soret number, and geometry parameters $a = a_1/d_1$, $b = a_2/d_2$, and $d = d_2/d_1$ satisfy the condition:

$$a^2+b^2+2ab\cos\phi\le(1+d)^2 \tag{32}$$

The dimensionless average flux in the wave frame F defined by:

$$F=\int_{h_2(x)}^{h_1(x)}\frac{\partial\Psi}{\partial y}\mathrm{d}y=\Psi[x,h_1(\xi)]-\Psi[x,h_2(x)] \tag{33}$$

which is related with dimensionless average flux in the laboratory frame θ, by the relation:

$$\theta = F + 1 + d \tag{34}$$

Solution of the problem

Equations (20)-(28) with boundary conditions (29) and (30) are solved using regular perturbation method. For perturbation solutions we expand the flow quantities in term of small wave number δ ($\delta \ll 1$), as:

$$\Psi = \sum_{i=0}^{\infty} \delta^i \Psi_i, \quad \mathbf{S} = \sum_{i=0}^{\infty} \delta^i \mathbf{S}_i, \quad \eta = \sum_{i=0}^{\infty} \delta^i \eta_i, \quad \varphi = \sum_{i=0}^{\infty} \delta^i \varphi_i, \quad Z = \sum_{i=0}^{\infty} \delta^i Z_i \tag{35}$$

After substituting eq. (35) into eqs. (20)-(28) with boundary conditions (29) and (30) and comparing the coefficients of powers of δ, we obtain the system of equations.

Zeroth order system

The zeroth order system is:

$$\frac{\partial^2 S_{0xy}}{\partial y^2} = 0 \tag{36}$$

$$\frac{1}{\mathrm{Pr}} \frac{\partial^2 \eta_0}{\partial y^2} + \mathrm{Ec}\Phi_0 = 0 \tag{37}$$

$$\frac{1}{\mathrm{Sc}} \frac{\partial^2 \varphi_0}{\partial y^2} + \mathrm{Sr} \frac{\partial^2 \eta_0}{\partial y^2} = 0 \tag{38}$$

$$S_{0xx} = 0, \quad S_{0xy} = 2\Psi_{0yy}, \quad S_{0yy} = 4\kappa \Psi_{0yy}^2, \quad \Phi_0 = 2\Psi_{0yy}^2 \tag{39}$$

$$\Psi_0 = \frac{F_0}{2}, \quad \frac{\partial \Psi_0}{\partial y} = -1, \quad \eta_0 = 0, \quad \varphi_0 = 0 \quad \text{at} \quad y = h_1(x) \tag{40}$$

$$\Psi_0 = -\frac{F_0}{2}, \quad \frac{\partial \Psi_0}{\partial y} = -1, \quad \eta_0 = 0, \quad \varphi_0 = 0 \quad \text{at} \quad y = h_2(x) \tag{41}$$

Substituting eq. (39) into eqs. (36)-(38) and then solving the resulting system, we obtain the solutions up to $O(\delta^0)$ as:

$$S_{0xy} = 4A_3 + 12A_4 y \tag{42}$$

$$\Psi_0 = A_1 + A_2 y + A_3 y^2 + A_4 y^3 \tag{43}$$

$$\eta_0 = S_1 + S_2 y + S_3 y^2 + S_4 y^3 + S_5 y^4 \tag{44}$$

$$\varphi_0 = S_{15} + S_{16} y + S_{17} y^2 + S_{18} y^3 + S_{19} y^4 \tag{45}$$

To calculate heat transfer coefficient at upper and lower wall (see [21]) we used:

$$Z_{0h_1} = \frac{\partial h_1}{\partial x} \times \frac{\partial \eta_0}{\partial y}, \quad Z_{0h_2} = \frac{\partial h_2}{\partial x} \times \frac{\partial \eta_0}{\partial y}$$

and obtained

$$Z_{0h_1} = a \cos x (S_2 + 2S_3 y + 3S_4 y^2 + 4S_5 y^3) \tag{46}$$

$$Z_{0h_2} = -b \cos(x + \phi)(S_2 + 2S_3 y + 3S_4 y^2 + 4S_5 y^3) \tag{47}$$

First order system

The first order system is:

$$\frac{\partial^2 S_{1xy}}{\partial y^2}+\frac{\partial^2 S_{0xx}}{\partial x\partial y}=\frac{\partial^2 S_{0yy}}{\partial x\partial y}+\mathrm{Re}(\Psi_{0y}\Psi_{0xyy}-\Psi_{0x}\Psi_{0yyy}) \tag{48}$$

$$\frac{1}{\mathrm{Pr}}\frac{\partial^2 \eta_1}{\partial y^2}+\mathrm{Ec}\Phi_1=\mathrm{Re}(\Psi_{0y}\eta_{0x}-\Psi_{0x}\eta_{0y}) \tag{49}$$

$$\frac{1}{\mathrm{Sc}}\frac{\partial^2 \varphi_1}{\partial y^2}+\mathrm{Sr}\frac{\partial^2 \eta_1}{\partial y^2}=\mathrm{Re}(\Psi_{0y}\varphi_{0x}-\Psi_{0x}\varphi_{0y}) \tag{50}$$

$$S_{1xx}=4\Psi_{0xy}+8\kappa\Psi_{0xy}^2 \tag{51}$$

$$S_{1xy}=2\Psi_{1yy}-2\kappa\Psi_{0y}\Psi_{0xyy}+2\kappa\Psi_{0x}\Psi_{0yyy}+4\kappa\Psi_{0xy}\Psi_{0yy} \tag{52}$$

$$S_{1yy}=8\kappa\Psi_{0yy}\Psi_{1yy}-4\Psi_{0xy} \tag{53}$$

$$\Phi_1=4\Psi_{0yy}\Psi_{1yy}-2\kappa\Psi_{0y}\Psi_{0yy}\Psi_{0xyy}+2\kappa\Psi_{0x}\Psi_{0yy}\Psi_{0yyy}+6\kappa\Psi_{0xy}\Psi_{0yy}^2-6\kappa\Psi_{0yy}\Psi_{0xy} \tag{54}$$

$$\Psi_1=\frac{F_1}{2},\quad \frac{\partial\Psi_1}{\partial y}=0,\quad \eta_1=0,\quad \varphi_1=0\quad \text{at}\quad y=h_1(x) \tag{55}$$

$$\Psi_1=-\frac{F_1}{2},\quad \frac{\partial\Psi_1}{\partial y}=0,\quad \eta_1=0,\quad \varphi_1=0\quad \text{at}\quad y=h_2(x) \tag{56}$$

Using zeroth order solutions eqs. (42)-(45) into the first order system eqs. (48)-(56) and then solving the resulting system, we obtain:

$$S_{1xy}=L_{37}+L_{38}y+L_{39}y^2+L_{40}y^3+L_{41}y^4+L_{42}y^5 \tag{57}$$

$$\Psi_1=B_1+B_2y+B_3y^2+B_4y^3+B_5y^4+B_6y^5+B_7y^6+B_8y^7 \tag{58}$$

$$\eta_1=S_6+S_7y+S_8y^2+S_9y^3+S_{10}y^4+S_{11}y^5+S_{12}y^6+S_{13}y^7+S_{14}y^8 \tag{59}$$

$$\varphi_1=S_{20}+S_{21}y+S_{22}y^2+S_{23}y^3+S_{24}y^4+S_{25}y^5+S_{26}y^6+S_{27}y^7+S_{28}y^8 \tag{60}$$

The heat transfer coefficient at upper and lower wall is calculated by the relations:

$$Z_{1h_1}=\frac{\partial h_1}{\partial x}\frac{\partial\eta_1}{\partial y},\quad Z_{1h_2}=\frac{\partial h_2}{\partial x}\frac{\partial\eta_1}{\partial y} \tag{61}$$

and obtained

$$Z_{1h_1}=a\cos x(S_7+2S_8y+3S_9y^2+4S_{10}y^3+5S_{11}y^4+6S_{12}y^5+7S_{13}y^6+8S_{14}y^7 \tag{62}$$

$$Z_{1h_2}=-b\cos(x+\phi)(S_7+2S_8y+3S_9y^2+4S_{10}y^3+5S_{11}y^4+6S_{12}y^5+7S_{13}y^6+8S_{14}y^7) \tag{63}$$

All coefficients appearing in the expressions of solutions are calculated by usual lengthy algebra that involved in regular perturbation method.

Discussion

The effects of viscoelastic parameter κ Reynold number Re, Prandtl number Pr, Eckert number Er, Soret number Sr, Schmidt number Sc, and phase difference ϕ appearing in solutions of the stream function Ψ, temperature distribution η, mass concentration field φ, and heat transfer coefficient Z are discussed and presented graphically in this section. Figures 2-11 present the effects of these parameters on the flow.

Figures 2 and 3 show the influence of κ and Re on shear stress S_{xy}. It is observed that shear stress is smaller near beginning and ending of the wave but becomes larger in the central region. Figures 2(a) and 2(b) show that at the upper (lower) wall, S_{xy} increases (decreases) in the first half of wave then decreases (increases) in the second half of wave with increasing κ. However, in figs. 3(a) and 3(b) it is depicted that at the upper (lower) wall shear stress decreases in the first half of wave whereas it increases (decreases) in the second half of wave with increasing Re.

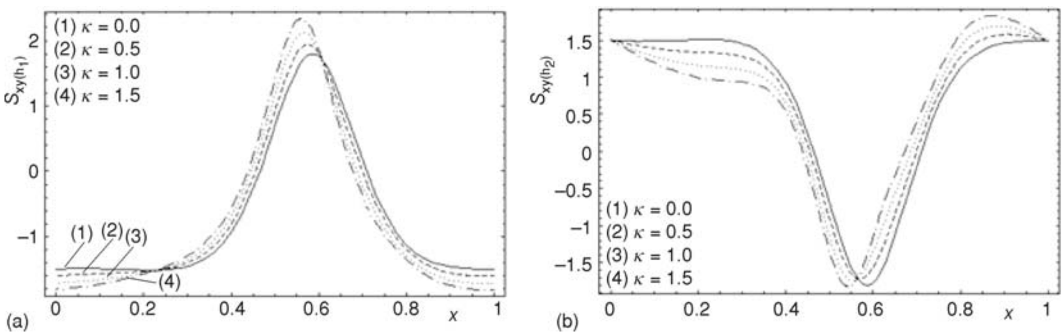

Figure 2. Effects of κ on (a) $S_{xy(h_1)}$ and (b) $S_{xy(h_2)}$ with x when a = 0.7, b = 1.2, d = 2, $\phi = \pi/6$, and θ = 1

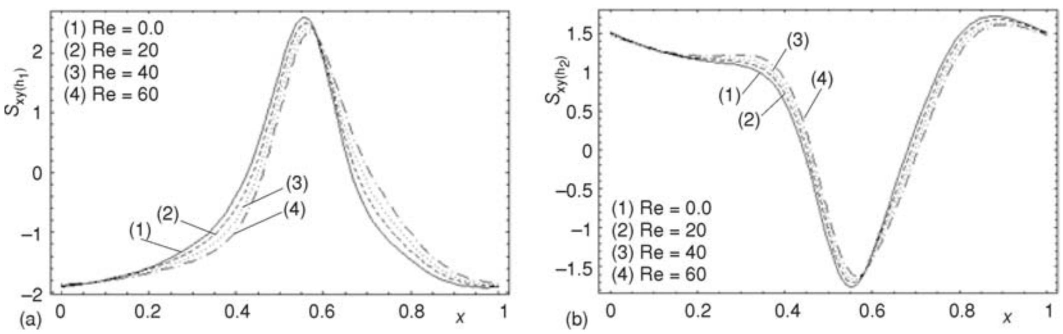

Figure 3. Effects of Re on (a) $S_{xy(h_1)}$ and (b) $S_{xy(h_2)}$ with x when a = 0.7, b = 1.2, d = 2, $\phi = \pi/6$, and θ = 1

Figures 4 and 5 display the temperature distribution η against y with the variation of parameters Ec, Pr, and θ. As anticipated, temperature profiles are almost parabolic concaved downward. These temperature profiles are greater near the upper wall which parabolically decreases moving toward the lower wall. It is worth to mention that in fig. 4(a) with the absence of viscous dissipation (Ec = 0) the temperature profiles are linear. Further, it is noticed in this fig-

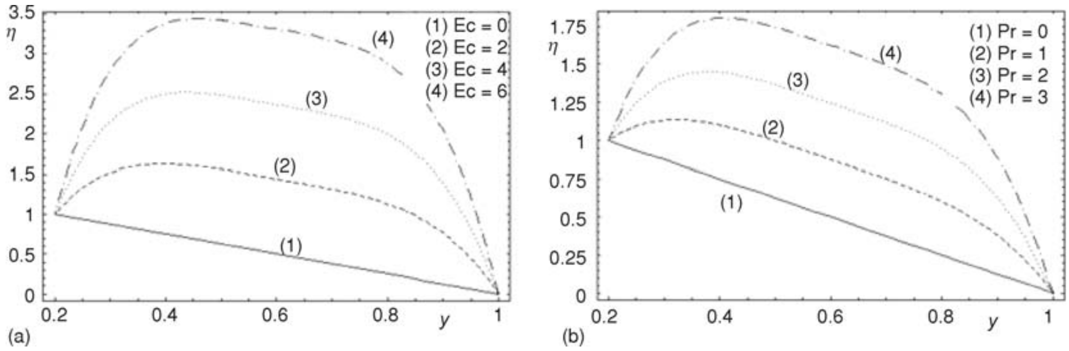

Figure 4. Temperature profile η for fixed a = 0.5, b = 1.2, d = 1, $\phi = \pi/2$, θ = 1, δ = 0.01, κ = 0.1, Re = 5, x = 0.5; (a) Pr = 5 and (b) Ec = 4

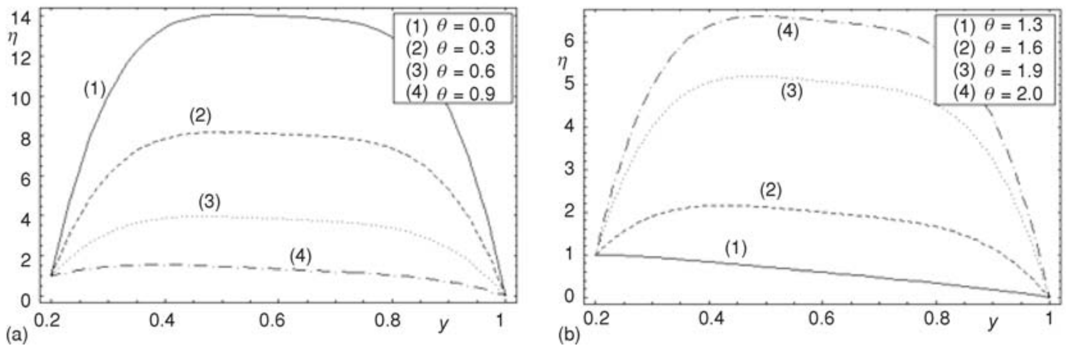

Figure 5. Temperature profile η for fixed a = 0.5, b = 1.2, d = 1, $\phi = \pi/2$, θ = 1, δ = 0.01, κ = 0.1, Re = 5, x = 0.5 Pr = 1, Ec = 4; (a) θ < 1; and (b) θ > 1

ure and fig. 4(b) that the temperature increases with increasing Pr and Er. Figure 5(a) shows that temperature decreases with increasing θ (θ < 1), whereas in fig. 5(b) it is seen that temperature increases with increasing θ (θ > 1).

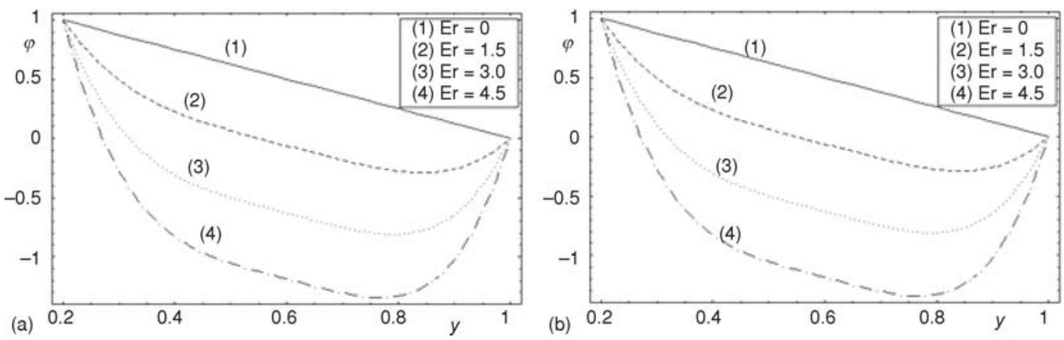

Figure 6. Concentration profile φ for fixed a = 0.5, b = 1.2, d = 1, θ = 1, $\phi = \pi/2$, δ = 0.01, κ = 0.1, Re = 5, x = 0.5, Sc = 1, Sr = 4; (a) Pr = 4; and (b) Ec = 4

Figures 6 and 7 portray the influence of Ec, Pr, Sc, and Sr on mass concentration φ. It is clearly observed that concentration field is parabolic concaved upward. This mass concentration φ is smaller near the lower wall which becomes larger moving towards the upper wall. It is noted that the variation in φ is less near the walls as compared to center of the channel. It is also noticed from these figures that φ decreases with increasing Ec, Pr, Sc, and Sr.

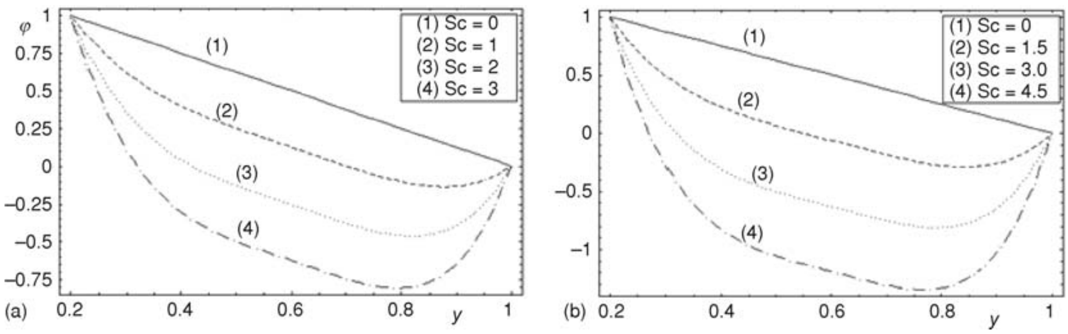

Figure 7. Concentration profile φ for fixed a = 0.5, b = 1.2, d = 1, θ = 1, ϕ = π/2, δ = 0.01, κ = 0.1, Re = 5, x = 0.5, Sc = 1, Sr = 4; (a) Pr = 4;(b) Ec = 4

Figures 8-11 present the coefficients of heat transfer Z_{h_1} and Z_{h_2} for different values of Ec, Pr, κ, and ϕ at upper and lower walls, respectively. Oscillatory behaviour is observed in all figures which is due to the propagation of peristaltic waves along the walls of the channel. Further, it is noticed that the absolute value of heat transfer coefficient increases with increasing Ec, Pr, and κ. It is also noted in fig. 11 that the absolute value of heat transfer coefficient increases at the upper wall but decreases at lower wall of the channel with increasing ϕ .

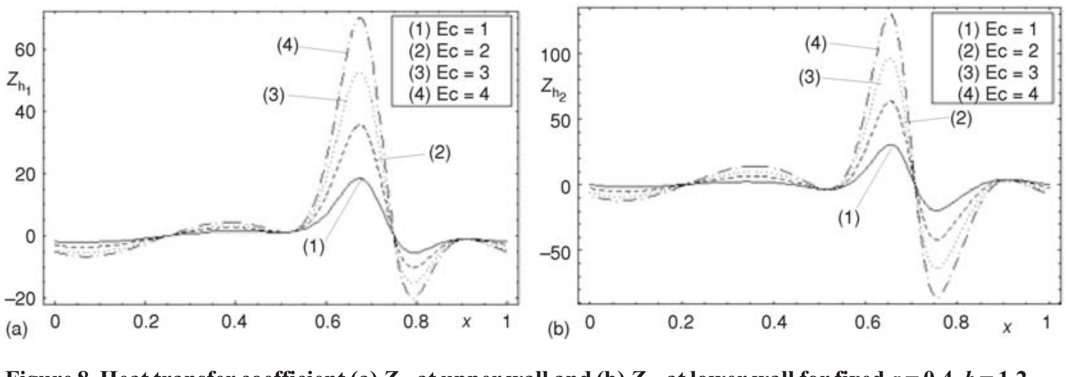

Figure 8. Heat transfer coefficient (a) Z_{h_1} at upper wall and (b) Z_{h_2} at lower wall for fixed a = 0.4, b = 1.2, d = 1.5, θ = 0.5, ϕ = π/12, δ = 0.01, κ = 0.1, Re = 5, Pr = 1

Conclusions

In this study, the problem of heat and mass transfer on peristaltic flow of Walter's B fluid in a two dimensional asymmetric channel is considered. The resulting equations are solved for small wave number using regular perturbation method. The solutions are analyzed and veri-

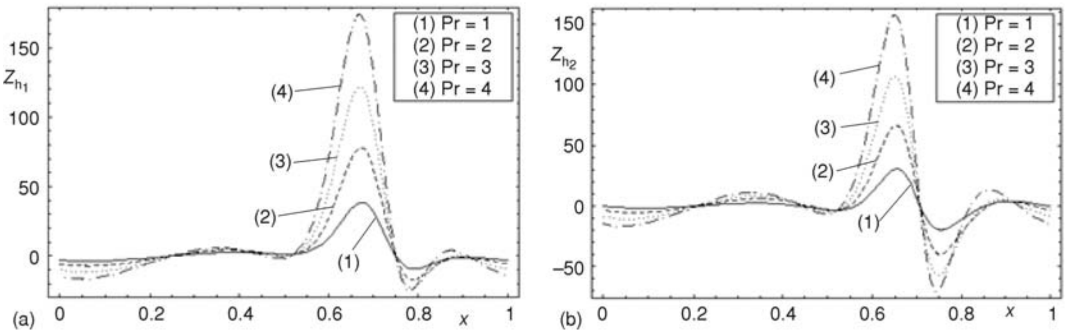

Figure 9. Heat transfer coefficient (a) Z_{h_1} at upper wall (b) Z_{h_2} at lower wall for fixed $a = 0.4$, $b = 1.2$, $d = 1.5$, $\theta = 0.5$, $\phi = \pi/12$, $\delta = 0.01$, $\kappa = 1$, Re = 1, Ec = 2

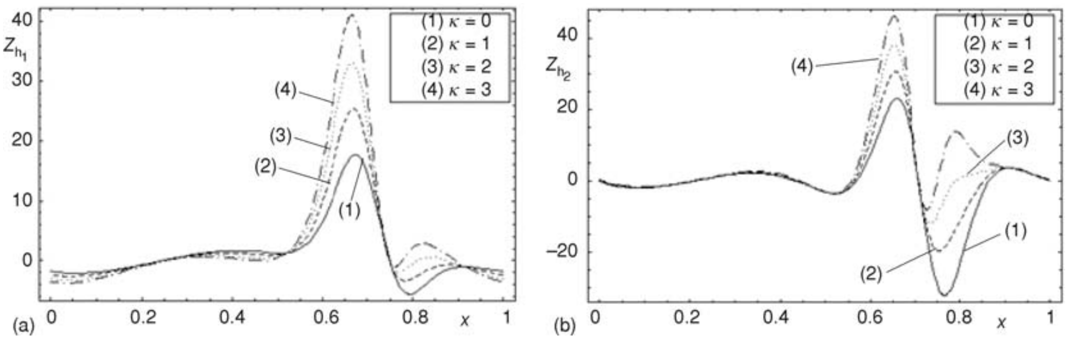

Figure 10. Heat transfer coefficient (a) Z_{h_1} at upper wall (b) Z_{h_2} at lower wall for fixed $a = 0.4$, $b = 1.2$, $d = 1.5$, $\theta = 0.5$, $\phi = \pi/12$, $\delta = 0.01$, Pr = 1, Re = 1, Ec = 2

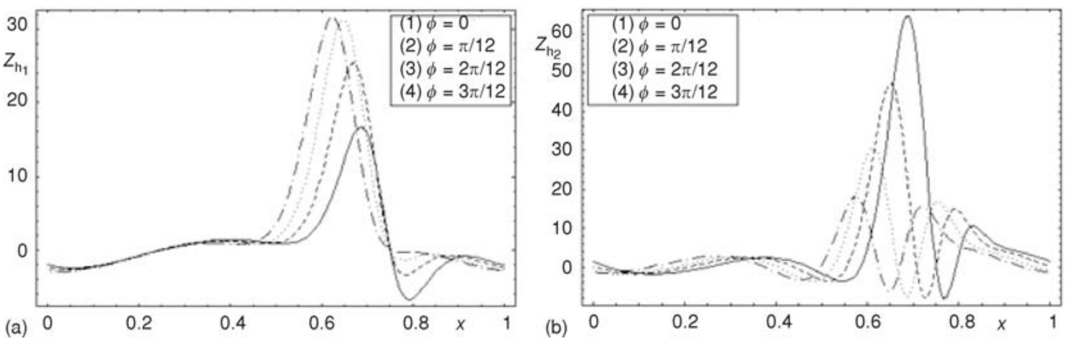

Figure 11. Heat transfer coefficient (a) Z_{h_1} at upper wall and (b) Z_{h_2} at lower wall for fixed $a = 0.4$, $b = 1.2$, $d = 1.5$, $\theta = 0.5$, k = 1, $\delta = 0.03$, Pr = 1, Re = 1, Ec = 1

fied graphically. It can be seen from the temperature and concentration profiles that the solutions obtained clearly satisfy the boundary conditions at upper ($\eta = 0, \varphi = 0$) and lower ($\eta = 1, \varphi = 1$) walls. Results show that the temperature and concentration profiles are parabolic and significant variations lie in the center of the channel due to viscous dissipation. In the absence of viscous dissipation and Soret effects, temperature and concentration profile becomes linear. Temperature of the fluid increases with increasing Eckert and Prandtl number while mass concentration decreases with increasing Soret and Schmidt number. On the other hand, the shear stress increases at the upper wall but decreases at lower wall with increasing κ. The behaviour of heat transfer coefficient is oscillatory which is due to propagation of peristaltic waves. As a limiting case of Newtonian fluid when $\kappa = 0$, $\delta = 0$, and Re = 0 our results reduce to those obtained by Mishra and Rao [30].

Acknowledgments

The authors would like to acknowledge Ministry of Higher Education (MOHE) and Research Management Centre UTM for the financial support through vote numbers 03J54, 78528 and 4F109 for this research.

References

[1] Shapiro, A. H., *et al*., Peristaltic Pumping with Long Wavelength at Low Reynolds Number, *J. Fluid Mech., 37* (1969), 4, pp. 799-825
[2] Beard, D. W., Walters, K., Elastico-Viscous Boundary-Layer Flows. Part I. Two-Dimensional Flow Near a Stagnation Point, *Proc. Camb. Phil. Soc., 60* (1964), 3, pp. 667-674
[3] Nandeppanavar, M. M., *et al*., Heat Transfer in a Walter's B Fluid over an Impermeable Stretching Sheet with Non-Uniform Heat Source/Sink and Elastic Deformation, *Commun. Nonlinear Sci. Numer. Simulat., 15* (2010), 7, pp. 1791-1802
[4] Joneidi, A. A., *et al*., Homotopy Analysis Method to Walter's B Fluid in a Vertical Channel with Porous wall, *Meccanica,45* (2010), 6, pp. 857-868
[5] Gupta, U., Aggarwal, P., Thermal Instability of Compressible Walter' (Model B) Fluid in the Presence of Hall Currents and Suspended Particles, *Thermal Science, 15* (2011), 2, pp. 487-500
[6] Nadeem, S., Akbar, N. S., Peristaltic Flow of Walter's B Fluid in a Uniform Inclined Tube, *J. Biorheol., 24* (2010), pp. 22-28
[7] Mehmood, O. U., *et al*., Peristaltic Transport of Walter's B Fluid in an Asymmetric Channel, *Int. J. Appl. Math. Mech., 7* (2011), 21, pp. 1-19
[8] Tripathi, D., *et al*., Influence of Slip Condition on Peristaltic Transport of a Viscoelastic Fluid with Fractional Burger's Model, *Thermal Science, 15* (2011), 2, pp. 501-515
[9] Tripathi, D., Peristaltic Flow of a Fractional Second Grade Fluid through a Cylindrical Tube, *Thermal Science, 15* (2011), Suppl. 1, pp. S167-S173
[10] Vries, K., *et al*., Contractions of the Inner Third of the Myometrium, *Am. J. Obstet. Gynecol., 162* (1990), 3, pp. 679-682
[11] Eytan, O., Elad, D., Analysis of Intra-Uterine Fluid Motion Induced by Uterine Contractions, *Bull. Math. Biol., 61* (1999), 2, pp. 221-238
[12] Dursunkaya, Z., Worek, W. M., Diffusion-Thermo and Thermal-Diffusion Effects in Transient and Steady Natural Convection from Vertical Surface, *Int. J. Heat Mass Transf., 35* (1992), 8, pp. 2060-2065
[13] Postelnicu, A., Influence of a Magnetic Field on Heat and Mass Transfer by Natural Convection from Vertical Surfaces in Porous Media Considering Soret and Dufour Effects, *Int. J. Heat Mass Transf., 47* (2004), 6-7, pp. 1467-1472
[14] Ogulu, A., Effect of Heat Generation on Low Reynolds Number Fluid and Mass Transport in a Single Lymphatic Blood Vessel with Uniform Magnetic Field, *Int. Commun. Heat Mass Transf., 33* (2006), 6, pp. 790-799
[15] Vajravelu, K., *et al.*, Peristaltic Flow and Heat Transfer in a Vertical Porous Annulus, with Long Wave Approximation, *Int. J. Non Linear Mech.,42* (2007), 5, pp. 754-759
[16] Srinivas, S., Kothandapani, M., Peristaltic Transport in an Asymmetric Channel with Heat Transfer – A note, *Int. Commun. Heat Mass Transf., 35* (2008), 4, pp. 514-522

[17] Beg, O. A., *et al*., Numerical Study of Free Convection Magnetohydrodynamic Heat and Mass Transfer from a Stretching Surface to a Saturated Porous Medium with Soret and Dufour Effects, *Comput. Mater. Sci., 46* (2009), 1, pp. 57-65
[18 Beg, O. A., *et al*., Free Convection Heat and Mass Transfer from an Isothermal Sphere to a Micropolar Regime with Soret/Dufour Effects, *Int. J. Heat Mass Transf., 54* (2011), 1-3, pp. 9-18
[19] Srinivas, S., *et al*., A Note on the Influence of Heat and Mass Transfer on a Peristaltic Flow of a Viscous Fluid in a Vertical Asymmetric Channel with Wall Slip, *Chem. Ind. Chem. Eng. Quart., 18* (2012), 3, pp. 483-493
[20] Muthuraj, R., Srinivas, S., Mixed Convective Heat and Mass Transfer in a Vertical Wavy Channel with Travelling Thermal Waves with Porous Medium, *Comput. Math. Appl., 59* (2010), 11, pp. 3516-3528
[21] Srinivas, S., *et al*., Mixed Convective Heat and Mass Transfer in an Asymmetric Channel with Peristalsis, *Commun. Nonlinear Sci. Numer. Simulat., 16* (2011), 4, pp. 1845-1862
[22] Srinivas, S., Muthuraj, R., Effects of Chemical Reaction and Space Porosity on MHD Mixed Convective Flow in a Vertical Asymmetric Channel with Peristalsis, *Math. Comput. Model., 54* (2011), 5-6, pp. 1213-1227
[23] Srinivas, S., *et al*., A Study on Thermal-Diffusion and Diffusion-Thermo Effects in a Two-Dimensional Viscous Flow between Slowly Expanding or Contracting Walls with Weak Permeability, *Int. J. Heat Mass Transf., 55* (2012), 11-12, pp. 3008-3020
[24] Eldabe, N. T. M., *et al*., Mixed Convective Heat and Mass Transfer in a Non-Newtonian Fluid at a Peristaltic Surface with Temperature-Dependent Viscosity, *Arch. Appl. Mech., 78* (2008), 8, pp. 599-624
[25] Hayat, T., Mehmood, O. U., Slip Effects on MHD Flow of Third Order Fluid in a Planar Channel, *Commun. Nonlinear Sci. Numer. Simulat.,16* (2011), 3, pp. 1363-1377
[26] Hayat, T., Hina, S., The Influence of Wall Properties on the MHD Peristaltic Flow of a Maxwell Fluid with Heat and Mass Transfer, *Nonlinear Anal. Real World Appl., 11* (2010), 4, pp. 3155-3269
[27] Akbar, N. S., *et al*., Effects of Heat and Mass Transfer on the Peristaltic Flow of Hyperbolic Tangent Fluid in an Annulus, *Int. J. Heat Mass Transf. 54* (2011), 19-20, pp. 4360-4369
[28] Nadeem, S., Akbar, N. S., Influence of Heat and Mass Transfer on the Peristaltic Flow of a Johnson Segalman Fluid in a Vertical Asymmetric Channel with Induced MHD, *J. Taiwan Inst. Chem. Eng., 42* (2011), 1, pp. 58-66
[29] Hayat, T., Hina, S., Effects of Heat and Mass Transfer on Peristaltic Flow of Williamson Fluid in a Non-Uniform Channel with Slip Conditions, *Int. J. Numer. Meth. Fluids, 67* (2011), 11, pp. 1590-1604
[30] Mishra, M., Rao, A. R., Peristaltic Flow of Newtonian Fluid in an Asymmetric Channel, *Zeit. Ang. Math. Phys., 54* (2003), 3, pp. 532-550

Paper submitted: September 18, 2011
Paper revised: May 9, 2012
Paper accepted: May 9, 2012